

Reflective polarization volume gratings for high efficiency waveguide-coupling augmented reality displays

YUN-HAN LEE,^{1,2} KUN YIN,^{1,2} AND SHIN-TSON WU^{1,*}

¹CREOL, The College of Optics and Photonics, University of Central Florida, Orlando, Florida 32816, USA

²These authors contributed equally to this work

*swu@ucf.edu

Abstract: We demonstrate a reflective liquid-crystal polarization volume grating with high efficiency for augmented reality displays. The coupling efficiency was measured to be 90% at 650 nm and 50° deflection angle. The angular dependence of reflection band agrees well with Bragg condition, and the transmittance of environment light is high with negligible scattering. The bandwidth can be tailored by controlling the layer periodicity, allowing versatile applications and design freedom not only for augmented realities but also for other photonic devices.

©2017 Optical Society of America

OCIS codes: (050.7330) Volume gratings; (090.2820) Heads-up displays; (160.3710) Liquid crystals.

References and links

1. B. C. Kress and W. J. Cummings, "Towards the ultimate mixed reality experience: HoloLens display architecture choices," *SID Int. Symp. Digest Tech. Papers* **48**(1), 127–131 (2017).
2. I. Kasai, Y. Tanijiri, E. Takeshi, and U. Hiroaki, "A practical see-through head mounted display using a holographic optical element," *Opt. Rev.* **8**(4), 241–244 (2001).
3. T. Levola, "Novel diffractive optical components for near to eye displays," *SID Int. Symp. Digest Tech. Papers* **37**(1), 64–67 (2006).
4. T. Rasmussen, "Overview of high-efficiency transmission gratings for molecular spectroscopy," *Spectroscopy (Springf.)* **29**(4), 32–39 (2014).
5. F. Bruder, T. Fäcke, R. Hagen, D. Hönel, E. Orselli, C. Rewitz, T. Rölle, and G. Walze, "Diffractive optics with high Bragg selectivity: volume holographic optical elements in Bayfol® HX photopolymer film," *Proc. SPIE* **9626**, 96260T (2015).
6. R. L. Sutherland, L. V. Natarajan, V. P. Tondiglia, and T. J. Bunning, "Bragg gratings in an acrylate polymer consisting of periodic polymer-dispersed liquid-crystal planes," *Chem. Mater.* **5**(10), 1533–1538 (1993).
7. Y. J. Liu and X. W. Sun, "Holographic polymer-dispersed liquid crystals materials, formation, and applications," *Adv. Optoelectron.* **2008**, 684349 (2008).
8. N. V. Tabiryan, S. V. Serak, D. E. Roberts, D. M. Steeves, and B. R. Kimball, "Thin waveplate lenses of switchable focal length-new generation in optics," *Opt. Express* **23**(20), 25783–25794 (2015).
9. K. Gao, C. McGinty, H. Payson, S. Berry, J. Vornehm, V. Finnemeyer, B. Roberts, and P. Bos, "High-efficiency large-angle Pancharatnam phase deflector based on dual-twist design," *Opt. Express* **25**(6), 6283–6293 (2017).
10. C. Oh and M. J. Escuti, "Achromatic diffraction from polarization gratings with high efficiency," *Opt. Lett.* **33**(20), 2287–2289 (2008).
11. X. Xiang, J. Kim, R. Komanduri, and M. J. Escuti, "Nanoscale liquid crystal polymer Bragg polarization gratings," *Opt. Express* **25**(16), 19298–19308 (2017).
12. Y. H. Lee, G. Tan, T. Zhan, Y. Weng, G. Liu, F. Gou, F. Peng, N. V. Tabiryan, S. Gauza, and S. T. Wu, "Recent progress in Pancharatnam-Berry phase optical elements and the applications for virtual/augmented realities," *Opt. Data Process. Storage* **3**(1), 79–88 (2017).
13. Y. Weng, D. Xu, Y. Zhang, X. Li, and S.-T. Wu, "Polarization volume grating with high efficiency and large diffraction angle," *Opt. Express* **24**(16), 17746–17759 (2016).
14. J. Kobashi, H. Yoshida, and M. Ozaki, "Planar optics with patterned chiral liquid crystals," *Nat. Photonics* **10**(6), 389–392 (2016).
15. J. Kobashi, Y. Mohri, H. Yoshida, and M. Ozaki, "Circularly-polarized, large-angle reflective deflectors based on periodically patterned cholesteric liquid crystals," *Opt. Data Process. Storage* **3**(1), 61–66 (2017).
16. J. Wang, C. McGinty, J. West, D. Bryant, V. Finnemeyer, R. Reich, S. Berry, H. Clark, O. Yaroshchuk, and P. Bos, "Effects of humidity and surface on photoalignment of brilliant yellow," *Liq. Cryst.* **5**(44), 863–872 (2017).

17. H. Mukawa, K. Akutsu, I. Matsumura, S. Nakano, T. Yoshida, M. Kuwahara, and K. Aiki, "A full-color eyewear display using planar waveguides with reflection volume holograms," *SID Int. Symp. Digest Tech. Papers* **17**(3) 185–193 (2009).

1. Introduction

Augmented reality (AR) displays, such as Microsoft HoloLens [1], are emerging rapidly in recent years. Such a see-through device overlays the environment and the displayed information with an optical combiner. To enable a slim design, waveguide-based combiners have been investigated [2, 3]. In this type of device, the display light is collimated and deflected into thin waveguides through an input-coupler. After traveling to the viewing region through total-internal reflection, the light is again deflected toward the observer's eye by an output-coupler. The input- and output-couplers are large-angle deflectors that are currently made with holographic volume gratings and surface-relieve gratings. Common holographic volume gratings are isotropic materials with alternative slanted layers of high and low refractive indices. The angular bandwidth for a single holographic volume grating is determined by the index contrast. As reported in [4], holographic volume gratings based on dichromated gelatin can provide an index contrast as high as 0.15; however, dichromated gelatin-based holographic volume gratings are sensitive to environmental conditions such as humidity and temperature, and are therefore unstable for commercial applications. Nowadays, most of the design adopted photo-polymers as recording media with index contrast around 0.035 [5]. As a result, the deflection has a high angle/wavelength selectivity. This allows almost 100% transmittance of the environment light; however, this also translates into a very low efficiency for the display light, causing a high power consumption. To widen the field of view while maintaining flat profile, multiple layers of holographic volume gratings are exploited. This not only reduces the transmittance but also greatly increases the device cost. The polarization-sensitive counterpart of holographic gratings, often referred to holographic polymer-dispersed liquid crystal (HPDLC) [6, 7], exploit electrically-responsive birefringent liquid crystal materials and therefore can allow switchable grating couplers with higher index contrast. Fabrication challenges exist for high quality holographic gratings and HPDLCs due to the inhomogeneity induced during the diffusion process, resulting in optical imperfections in the structure [7]. Surface-relieve gratings, on the other hand, exploiting alternate air-polymer slanted structure, and therefore can theoretically achieve a higher index contrast with better efficiency and large angular acceptance. However, it is challenging to achieve ideal optical efficiency in mass production due to the difficulty in replicating oblique high-aspect-ratio grooves [3].

Recently, extensive work has been attempted to applying Pancharatnam-Berry deflectors (PBDs) for waveguide coupling [8–15]. The transmissive PBDs show promising high efficiency and are relatively easy to fabricate, in comparison with surface-relieve gratings. However, the transmissive PBDs will partially diffract the ambient light into the observer's eye and therefore are more suitable to work as input-couplers rather than output-couplers. Reflective PBDs, due to their physical properties, are also referred to as reflective polarization volume gratings (reflective PVGs). They reflect the environment light away from the observer's eye and provide clear cut-off wavelength similar to reflective holographic volume gratings, and therefore are more suitable for output-couplers. The polarization dependency also allows for higher coupling efficiency. The pioneering work on reflective PBDs has been done by Kobashi et al [14, 15], and yet the deflection angle and the efficiency are still limited and insufficient for applications in AR waveguides.

In this paper, we experimentally demonstrate a high efficiency, large deflection angle waveguide coupler based on reflective PVGs. In a reflective PVG, liquid crystal (LC) is aligned in a helical twist with helix axis vertical to the substrate, as shown in Fig. 1(a). The in-plane periodicity Λ_x from the alignment layer and the vertical periodicity Λ_y (helical pitch $P = 2\Lambda_y$) are related to the Bragg periodicity Λ_B as:

$$\begin{cases} \Lambda_x = \Lambda_B / \sin \phi \\ \Lambda_y = \Lambda_B / \cos \phi \end{cases} \quad (1)$$

where ϕ corresponds to the slant angle, which is the angle between the grating vector \mathbf{k} and the vertical axis, as denoted in Fig. 1(a). The slow-axis of LC directors, represented as the long axis of ellipsoids in Fig. 1(a), $\rho(x, y)$ which is uniform along z-axis can be expressed as follows:

$$\rho(x, y) = \frac{\pi}{\Lambda_x} x + \frac{\pi}{\Lambda_y} y. \quad (2)$$

A proper helical period should be chosen to allow the highest deflection efficiency at designated wavelength. The deflection central wavelength λ_B is described by:

$$\lambda_B = 2n_{\text{eff}}\Lambda_B \cos \theta, \quad (3)$$

where θ represents the incident angle with respect to the slant angle (e.g., at normal incidence, $\theta = \phi$), n_{eff} is the effective refractive index, with $n_{\text{eff}} = \sqrt{(n_e^2 + 2n_o^2)}/3$, and n_e and n_o are the extraordinary and ordinary refractive indices, respectively.

Equations (1) and (3) are similar to those of holographic gratings, indicating that reflective PVGs in its essence resembles a slanted multi-layer structure for circularly polarized light with the same handedness as the helical twist. Due to the inherent high index contrast (>0.15), these reflective PVGs provide high efficiency with large reflection bandwidth. The thickness of PVG layer is directly related to the efficiency, as simulated through finite-element method (FEM) [13]. As shown in Fig. 1(b), the 3- μm thick PVG effectively deflects 95% of the incident light. We experimentally verified the relation between coupling efficiency and thickness of the PVG film and investigated the spectral behavior at different thickness and incident angle. We validated the possibility to extend the bandwidth through multi-helical periodicity and demonstrated a wide band deflection PVG. The angular behaviors were also investigated.

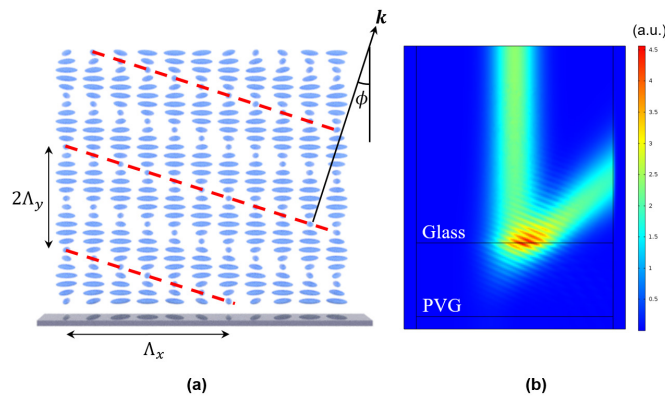


Fig. 1. (a) The schematic plot of a reflective PVG with in-plane periodicity denoted as Λ_x , vertical periodicity as Λ_y (helical pitch $P = 2\Lambda_y$), the grating vector as \mathbf{k} , and the slant angle being ϕ . For a normal incidence, the deflection angle is 2ϕ . (b) The FEM simulation with a circularly polarized light entering from glass onto a 3- μm thick PVG layer at normal incidence ($\Delta n = 0.18$, $\Lambda_x = 540$ nm, $\Lambda_y = 250$ nm and $\lambda = 650$ nm).

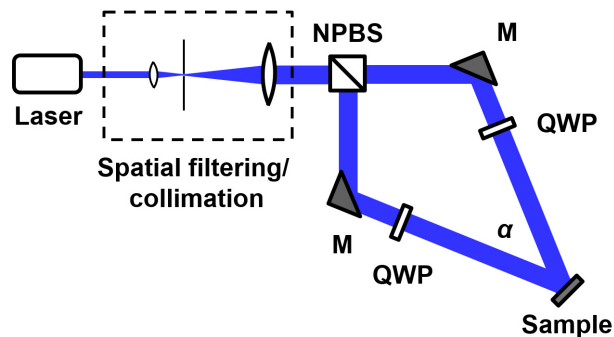


Fig. 2. The setup for interference exposure process. The beam from linearly polarized He-Cd laser was filtered, collimated and split into two paths with a non-polarizing beam splitter (NPBS). They were then sent through quarter wave plates (QWPs) to form two opposite-handed circularly polarized light beams and interfere at an angle of $\alpha = 55^\circ$ at the sample.

2. Experimental

To fabricate reflective PVGs, we spin-coated photo-alignment material Brilliant yellow (0.4 wt%) dissolved in dimethylformamide (DMF) [16] onto cleaned glass substrates at 800 rpm for 5 s and then 3,000 rpm for 30 s to create uniform thin films on the substrates. The films were dried on a hotplate at 120 °C for 30 minutes. These substrates were then subjected to the 442-nm interference exposure (He-Cd laser, Kimmon). The optical setup is shown in Fig. 2.

The beam from a linearly polarized He-Cd laser was split into two paths with a non-polarizing beam splitter (NPBS). They were then sent through a quarter-wave plate (QWP) to generate two opposite-handed circularly polarized beams. These two beams were aligned to make an angle $\alpha = 55^\circ$ onto the coated substrate to generate a periodicity $\Lambda_x \cong 540$ nm. The exposure dosage was 3 J/cm². The chiral twist LC polymer precursor consists of 1.47 wt% of R5011, 5 wt% of Irgacure 651 and 93.6 wt% of RM257 to generate a vertical periodicity $\Lambda_y \approx 250$ nm. It was diluted in toluene at 1:9 in weight and was spin-coated onto the exposed substrates at 2000 rpm for 30 s. The coated substrate was then cured with UV light at a dosage of 2.5 J/cm² in nitrogen environment. Then it was repeatedly coated and cured until sufficient thickness was achieved. To measure the diffraction efficiency, we placed the sample on a spectrometer with circularly polarized light at normal incidence. The spectra were normalized to that of a blank glass slide. It is confirmed that minimal scattering loss exists since the transmittance outside the reflection bandwidth approaches 100%. Therefore, the decreased transmission is attributed to the deflection efficiency of PVG. To simulate the PVG properties, we exploit a rigorous model based on FEM using the COMSOL Multiphysics, which is a commercial finite element package [13].

3. Results and discussion

Figure 3 shows the relation between total thickness of PVG film and the coupling efficiency. The theoretical analysis shows that the efficiency approaches 100% at 4 μm , and becomes insensitive to film thickness beyond 4 μm (i.e., it maintains nearly 100%). As expected, the experimental result showed that the efficiency grows monotonically as the thickness increases, and the coupling efficiency reaches 90% when the thickness increases to 2.9 μm . Although the experimental result is slightly lower than that expected from simulation, the trend largely agrees. The main contribution to the slight discrepancy is presumably the non-perfect helix structure, since when spin-coated, the upper boundary of the LC layer is not anchored. Therefore, the effective good-alignment region may be slightly thinner than the measured one. As indicated in Fig. 3, the efficiency can be further increased to approaching 100% by increasing the thickness to 4-5 μm . It is important to note that the efficiency is only for circularly polarized input and the opposite circular polarization can fully transmit through

the PVG. This provides high transmittance of the ambient light which is especially important for the see-through optics. The inset of Fig. 3 is a photo taken under room light (at roughly 25° incident angle) showing the reflection of a $2.9\text{-}\mu\text{m}$ sample at roughly 55° , because the light will be guided into the glass substrate at normal angle. The PVG region was marked with a blue enclosure. The PVG region appears orange at this specific angle, and the apparent deflection color varies at different viewing angles. The angular dependency will be discussed in the latter section.

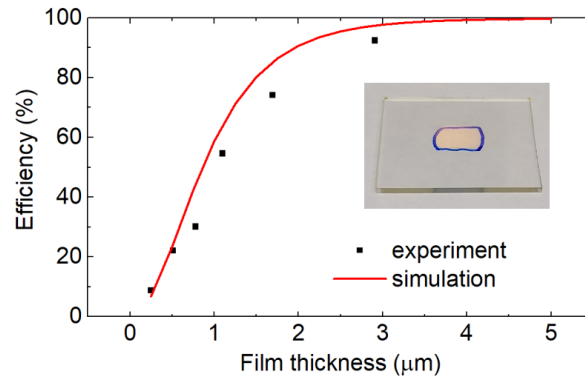


Fig. 3. Measured and simulated diffraction efficiency at $\lambda = 650\text{ nm}$ and different thickness of PVG film. A fair agreement is observed. Inset: a $2.9\text{-}\mu\text{m}$ sample viewed from an oblique angle with the PVG region circled by the blue line.

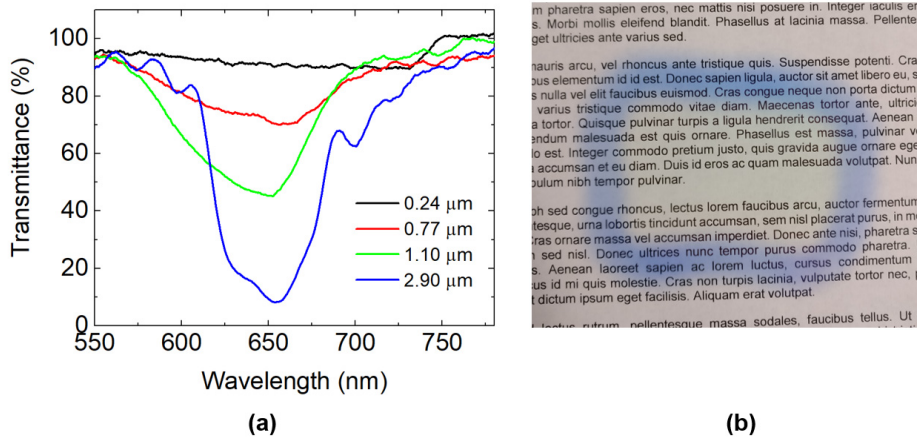


Fig. 4. (a) The transmission spectra for PVG samples with different film thickness. The deflection angle (in glass) was roughly 50° at 650 nm . A clear reduction in bandwidth is observed, while the reflection efficiency increases significantly as the thickness increases to $2.9\text{ }\mu\text{m}$. (b) A photo taken through the PVG sample with $2.9\text{-}\mu\text{m}$ thickness. PVG region is circled in the blue line. The distance between PVG to camera was 1 cm , and the target was 10 cm away.

Figure 4(a) depicts the measured transmission spectra at different PVG thicknesses with a circularly polarized light. The major contribution in transmission drop may originate from beam deflection of PVG, scattering and absorption. While the former is centered at Bragg wavelength (here at 650 nm), the latter two usually have broader bandwidth. From the high transmittance in side band (say, around 560 nm), we find that the scattering and absorption are very minimal. As the thickness increases, the reflection bandwidth decreases while the efficiency increases. As the thickness approaches $3\text{ }\mu\text{m}$, a clear reflection band is formed with its central wavelength located at around 650 nm . The peak efficiency was roughly 90% .

Figure 4(b) shows a photo taken through the 2.9- μm sample. The distance between PVG to camera was 1 cm, and the target was 10 cm away. The clear image seen through the PVG region (in blue enclosure) indicates low scattering of the PVG film. Due to the handedness selectivity, at the reflection band, this allows more than 50% transmission of the ambient light even when the circularly polarized input was out-coupled at 90% efficiency. This along with the clear cut-off in reflection bandwidth allows high transmission and therefore the background can still be clearly seen. As the light in the reflection band does not travel to the observer's eye, this also avoids ghost imaging, as oppose to the case of transmissive PVGs.

The angular dependent reflection band was measured as Fig. 5(a) shows. As the incident angle increases from 0° to 20° , the bandwidth shifts toward shorter wavelength, and when the angle decreases to -20° , the bandwidth shifts toward the longer wavelength side. The asymmetry is introduced through the slanted structure similar to the case of conventional holographic gratings. The corresponding angular spectrum at 650 nm is shown in Fig. 5(b). The angular dependency is plotted in Fig. 6 in terms of the shift in maximum reflection wavelength. The shift in wavelength fits well with Eq. (3). The angular dependency results in color shift of the display image after propagating toward the viewing region, and it is therefore important to optimize the bandwidth properly by controlling the birefringence of the employed liquid crystal material and to compensate the colors through software methods [17].

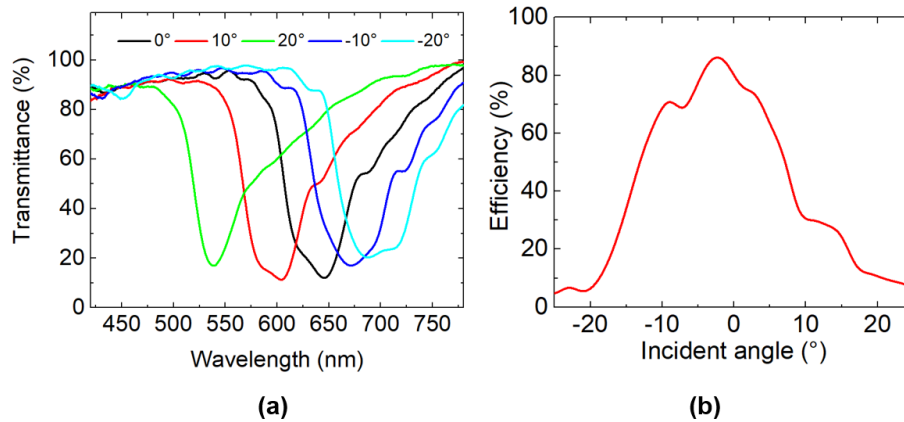


Fig. 5. (a) Measured transmission spectra of a PVG sample at different incident angles (from air). (b) Measured deflection efficiency at 650 nm at different incident angle (from air).

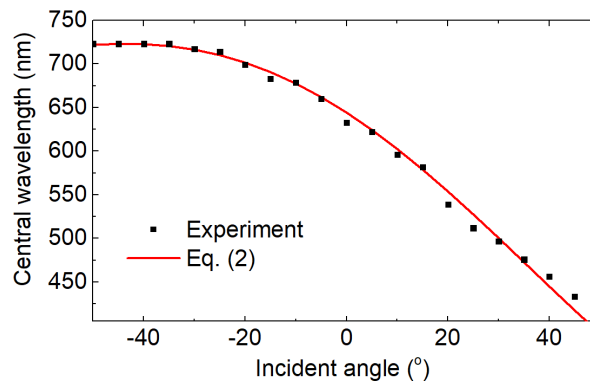


Fig. 6. The central wavelength versus the incident angle (from air).

For augmented reality couplers, it is desirable to have a finite bandwidth to prevent cross-talk between red, green and blue waveguides. Yet for general optics and photonic applications, wide bandwidth may be desirable. The ability to control the composition in each

coated LC layer allows us to engineer the desired spectral behavior for reflective PVGs and extend the reflection bandwidth. By coating the LC precursor with three different concentrations of chiral materials (in this case, 1.4 wt%, 1.8 wt% and 2.2 wt%, each coated for 5 layers with the 1.8wt% and 2.2 wt% precursors further diluted to 1:19 in Toluene). As shown in Fig. 7, the three-period sample exhibits a wider reflection band. The band centered at ~ 500 nm is the overlapped result from the precursors with 1.8 wt% and 2.2 wt% chiral materials, while the reflection band centered at ~ 675 nm originates from the precursor with 1.4 wt% chiral material.

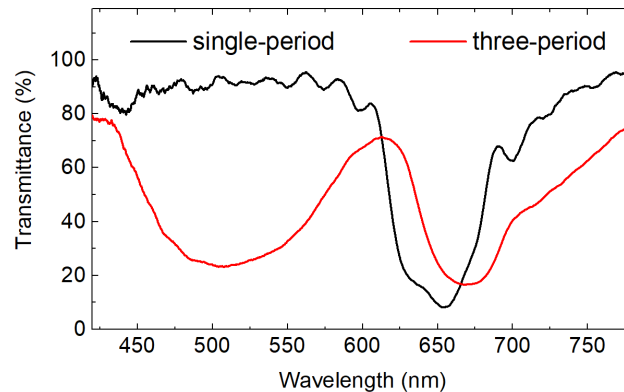


Fig. 7. The spectra of the single-period (single periodicity along vertical axis) sample and three-period sample, showing the capability to extend the reflection band using this fabrication process.

4. Conclusion

We have experimentally demonstrated a high-efficiency beam deflection and coupling with reflective PVGs. The efficiency is 90% with an in-glass deflection angle of 50° at $\lambda = 650$ nm. By increasing the film thickness, the efficiency can be increased to over 95%. The angular dependent Bragg reflection agrees well with theory, and the reflection spectra can be engineered by controlling the helix period for each layer. We demonstrated a three-period PVG with a wide reflection band covering red, green and blue regions. The fabricated reflective PVGs show high efficiency and optical clarity and it has good potential for waveguide coupling applications in augmented reality couplers and other photonic devices.

Funding

Air Force Office of Scientific Research (AFOSR) (FA9550-14-1-0279).